The International Journal of Advanced Manufacturing Technology
https://doi.org/10.1007/s00170-024-14439-1

ORIGINAL ARTICLE

# Analyzing and enhancing the porthole die design for extruding a complicated AA7005 profile

Thanh-Cong Nguyen[1,2] · Tat-Tai Truong[3] · Jun-Wei Wang[1] · Jinn-Jong Sheu[4] · Chih-Lin Hsu[5] · Quang-Cherng Hsu[1]

Received: 9 February 2024 / Accepted: 6 September 2024


## Abstract
Porthole extrusion enables the production of aluminum profiles with intricate cross-sections. It can efficiently shape complex profiles; however, few studies have investigated complex hot extrusions using porthole dies, particularly with 7000-series aluminum alloys. Although 7000-series aluminum alloys are renowned for their superior strength, they have poor extrudability, especially for complex extrusion profiles. Implementing an effective die design is essential for avoiding extrusion defects and maximizing extrusion performance. In this study, a porthole extrusion method for a complex profile was developed for AA7005, a medium–high-strength aluminum alloy. Computer-aided engineering simulations were employed to analyze die strength and forecast the flow of the material. After the first trial with the initial design, the lower die was slightly modified. However, following this minor modification, there were occurrences of material blockages. A major revision of die design was then performed, in which bearing length, die runout, and pocket shape were all adjusted. For validation, extrusion testing was conducted, and the effectiveness of the modifications was determined. Finally, the extrusion processes of the modified and initial die designs were compared, including their metal flow behavior, maximum extrusion forces, and product dimensions. The study highlights a well-rounded methodology that incorporates simulation and empirical results to comprehensively understand the challenges of complicated profile extrusion processes with medium–high-strength aluminum alloy.

**Keywords** Extrusion · Porthole die · Complicated profile · AA7005 · Medium–high-strength aluminum alloy · Extrusion simulation · Die design enhancement

## 1 Introduction

Aluminum alloys play a crucial role in many modern applications because of their excellent properties, such as their high strength-to-density ratio, formability, and recyclability. Extrusion is a method of shaping aluminum alloys into functional parts that can achieve a high production rate, favorable dimensional accuracy, and a wide variety of shapes. Because of their desirable properties and ease of processing, aluminum alloys are irreplaceable in various industries, including the automotive, aerospace, and construction industries [1–4]. Extruded aluminum alloys are often used in complicated structures because of their light weight, durability, weather resistance, design flexibility, and low cost. Demand for these alloys is primarily driven by the construction industry [5, 6], especially for applications aiming for sustainability and energy efficiency [7]. While 6000-series aluminum alloys were commonly used for complex extrusion profiles, such as the curtain structure [8], 7000-series alloys are gaining attraction due to their superior properties. This trend

✉ Quang-Cherng Hsu
hsuqc@nkust.edu.tw

1 Department of Mechanical Engineering, National Kaohsiung University of Science and Technology, 415 Chien-Kung Road, Kaohsiung City 80778, Taiwan

2 School of Mechanical and Automotive Engineering, Hanoi University of Industry, No. 298, Cau Dien Street, Bac Tu Liem District, Hanoi 11950, Vietnam

3 Department of Mechanical Engineering, Hung Yen University of Technology and Education, Dan Tien, Khoai Chau, Hung Yen 17817, Vietnam

4 Department of Mold and Die Engineering, National Kaohsiung University of Science and Technology, 415 Chien-Kung Road, Kaohsiung 80778, Taiwan

5 Gomore Building Envelope Technology Ltd, Wenhu St., Neihu Dist, Taipei 10607, Taiwan

Published online: 17 September 2024

is driven by the growing demand for complex structures that are compact, high-performance, and able to withstand natural disasters. However, challenges such as high cost and machining difficulty must be considered. These are expected to be overcome by technological and manufacturing development, thereby establishing 7000-series alloys as the common materials for complicated structures in extrusion.

Conventionally, extrusion dies were designed by experts based on empirical knowledge. However, this has been largely replaced by data-driven approaches that are supported by computer-aided engineering (CAE) simulation tools. These tools facilitate the virtual simulation of the extrusion process, enhancing precision and enabling the exploration of intricate geometries. However, this relies on the existing accumulated experiences to establish the necessary variables for the simulation. The scarcity of scholarly literature on extrusion die design for complicated high-strength aluminum alloy profiles presents difficulties when employing simulation in this work. Hence, employing a versatile collaboration of experimentation and simulation is inevitable to deal with this issue.

Researchers have focused on improved die designs and process analyses to increase the sustainability and efficiency of manufacturing. Advancements in computer-aided design, finite element analysis, and finite volume method [9–11] have enabled precise simulations of metal flow and stress distribution within the die, leading to optimized die designs and improved process parameters. Wang et al. [12] investigated the impact of the extrusion die design on material flow and product quality for AA6N01 large-scale aluminum alloy profiles. This study focuses on optimizing spread die and container structures to enhance material distribution and reduce die stress for a hollow, flat-wide profile used in high-speed trains. Qian et al. [13] developed an extrusion process for manufacturing complex, thin-walled AA6061 components with I-type longitudinal ribs. By optimizing die design and controlling metal flow, the study seeks to overcome challenges associated with traditional manufacturing methods and achieve high-quality, seamless components. Wang et al. [14] focused on optimizing porthole die design for manufacturing multi-cavity, thin-walled 6063 aluminum alloy profiles. The study investigates metal flow, seam weld strength, and die strength by introducing a novel combined porthole die and employing numerical simulations. Through structural modifications and experimental validation, the research aims to improve extrusion quality by balancing metal flow, enhancing weld integrity, and ensuring die durability. Another study investigated the impact of process parameters on the extrusion of aluminum alloy rims [15]. The finite element model was developed to simulate the hot extrusion process and analyze the influence of various factors on velocity distribution and extrusion pressure. The optimal process parameters for 7075 aluminum alloy rim profiles were determined through a Taguchi test and gray correlation analysis, aiming to enhance product quality and reduce energy consumption. Liu et al. [16] tackled the challenge of large, flat, thin-walled profiles in AA6060 through a novel spreading pocket die design. Virtual simulations and real trials have both revealed that optimized die structures can achieve significantly improved material flow uniformity, leading to higher quality extrusions and a more efficient overall process. Furthermore, an additional research effort [17] is dedicated to addressing the challenges related to the high length-to-width ratios and small cavities in AA6063 profiles. An innovative porthole die design was presented that significantly improved flow velocity, uniformity, temperature distribution, welding pressure, and die strength; the design was validated through both simulations and real-world experiments. Kathirgamanathan and Neitzert [18] researched uniform metal flow and surface quality for complex profiles. They used aluminum 6061 and 7075 as the extruded materials and investigated the effects of pocket shape, depth, location, and bearing length on flow behavior to better understand the effects of these parameters on the extrusion process. Truong et al. [19, 20] optimized die designs for complex AA6063 aluminum profiles. In their first study [19], they used FEA simulations to refine a specific porthole die design to improve flow balance and reduce stress for complex heatsinks. Their second study [20] was a broad investigation that employed comparative simulations to assess and optimize three die types (flat, pocket, and spread) for diverse profile requirements. Despite these differing approaches, both studies shared the common goal of improving extrusion efficiency and effectiveness by providing valuable insights for designers and engineers. Hsu et al. [21] explored advancements in hot extrusion of porthole-type extrusion dies for complex hollow profiles. Through a combined approach of finite element analysis and the Taguchi method, they successfully optimized a porthole-type die for non-symmetric hollow profiles by exploring pocket geometry and bearing length. Their optimized design, featuring a double arc type welding chamber pocket and unequal bearing length, minimized dead metal zones and achieved uniform material flow, as validated by successful extrusion trials. These studies demonstrate the ongoing efforts to refine and optimize extrusion processes for diverse and demanding material applications.

Aluminum extrusion has been researched extensively; however, few studies have investigated complex profile extrusion for high-strength aluminum alloys, especially 7000-series alloys. Although numerous studies have investigated complex profiles extrusion, they typically use 6000-series alloys, which are easier to extrude. Moreover, studies on high-strength alloys often concentrate on simpler profile geometries because of the inherent challenges associated with their superior mechanical properties. Research on the combined problem of applying high-strength 7000-series alloys to form complex profiles is lacking. Successfully extruding intricate profiles with these demanding materials requires investigating the complex interplay between material properties, die design, and process parameters. This study tackles the challenge of extruding complex profiles by focusing on aluminum curtain structure frames as a representative case. Building upon established principles of material flow, the authors propose an appropriate die design. To evaluate the die's effectiveness, the die was tested in real-world experiments and using comprehensive virtual simulations with CAE software. This combined approach ensures a thorough evaluation of the die's performance in handling the intricacies of aluminum structure extrusion.

An initial design was modified to change the pocket shape, size, bearing length, and die runout on the basis of the principles of optimal material flow. To assess the effectiveness of these adjustments, the initial and optimized designs were comprehensively compared in terms of their metal flow characteristics, die strengths, and extrusion force requirements. This thorough evaluation provided valuable insights regarding the effects of the modifications.

## 2 Materials and methods

Complexity is a critical metric for assessing the degree of difficulty of extruding a given profile. Extrudability tends to decrease as the profile perimeter increases, die diameter increases, or minimum product thickness decreases. These empirical observations have driven the development of various definitions of the complexity within the extrusion area [22, 23]. A commonly used method for quantifying the complexity of hollow sections is to calculate the ratio between the diameter of the circumscribing circle (DCC) and the minimum wall thickness of the profile ($T_{min}$) [24]:

$$\text{Complexity Index: CI} = \frac{\text{DCC}}{T_{min}} \quad (1)$$

In the present study, to validate the complexity index of the extrusion profile, complexity index calculations were performed for several profiles from the literature (Table 1). Clearly, lower complexity structures often use 6000-series alloys, and high-strength 7000-series alloys are selected for simpler geometries. By contrast, in this study, the extrusion of an intricate, high-complexity profile was investigated for a high-strength 7000-series aluminum alloy; specifically, porthole extrusion was performed. Figure 1 presents the extrusion profile in this study and its basic dimensions.

The target material, AA7005, a medium–high-strength alloy from the 7000 series, posed unique challenges due to its demanding extrusion requirements. To address these challenges, the research investigated the viability of utilizing H13 tool steel for the extrusion die, aiming to develop a die design capable of effectively handling the extrusion of 7000-series aluminum alloys with a readily available and potentially cost-effective die material. The mechanical and thermal properties of AA7005 and H13 are listed in Table 2.

**Table 1** Complexity index of profiles and their materials in related studies

| Profile | Complexity index (CI = DCC/ $T_{min}$) | Material |
|---|---|---|
| Curtain wall structure (this study) | 125 | AA7005 |
| Thin-walled with I-type ribs [13] | 27 | AA6061 |
| Heatsink profile [19] | 65 | AA6063 |
| Large-size, flat-wide, multi-ribs profile [17] | 81 | AA6060 |
| Thin-walled profile [14] | 95 | AA6063 |
| Large-scale profile [20] | 122 | AA6063 |
| Large-size, hollow, flat-wide profile [12] | 193 | AA6N01 |
| Solid profile with tips and thin walls [25] | 9 | AA7075 |
| Non-symmetric hollow profile [21] | 23 | AA7075 |
| Hollow rims [15] | 60 | AA7075 |

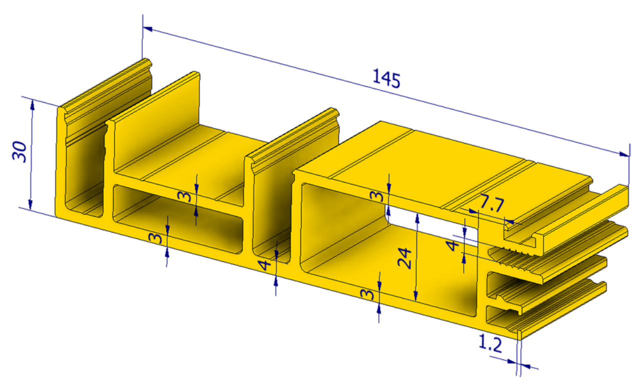


**Fig. 1** Dimensions of 3D model of desired profile (unit, millimeter)

### 2.1 Die design process

The porthole die design process in this study is presented as a flowchart in Fig. 2. The initial stage of designing a porthole extrusion die is accounting for material shrinkage during the cooling and solidification phases after extrusion. This was achieved by scaling the desired product profile by a factor of 1.01 [2, 16]. The die was then selected in accordance with the geometry of the product cross-section. In this case, a hollow profile was desired; therefore, a hollow die style was selected. The base die size for the aluminum alloy extrusion

**Table 2** Mechanical properties of AA7005 aluminum alloy and H13 steel

| Materials | AA7005 | H13 |
|---|---|---|
| Density (kg/m$^3$) | 2770 | 7870 |
| Specific heat (J/kg-K) | 900 | 460 |
| Young's modulus (Pa) | $4\times10^{10}$ | $2.1\times10^{11}$ |
| Poisson's ratio | 0.35 | 0.35 |
| Tensile strength (MPa) | 350 | 1400* |
| Yield strength (MPa) | 290 | 1300* |

*At 460 °C [26]

experiment was selected on the basis of the billet size and material strength.

For 7-inch billets, a larger die size should be chosen to improve the stability and strength during the extrusion process. Therefore, the largest practical option of 350 mm × 180 mm was chosen. Additionally, the backer die thickness was determined in accordance with the extruder in the experiment; therefore, a thickness of 160 mm was selected. This ensured compatibility and adequate support for the extrusion forces involved. These base and backer die sizes can achieve optimal performance and minimize the potential risks associated with medium-strength or high-strength aluminum alloy extrusion on smaller die configurations. A six-hole layout was selected for the porthole extrusion die to prioritize both flow control and die rigidity. This approach facilitated improved material flow toward the welding chamber and minimized the risk of bridge cracking during extrusion. While this decision led to more welding lines and increased processing complexity, it also offered valuable advantages. Besides, the large inlet diameter, exceeding 95% of the container diameter, effectively prevented surface oxide contamination from entering the die cavity. Additionally, the product center was positioned off-center relative to the die center. The die bridge design was selected to maximize the efficiency of material flow and weldability. This was achieved by employing a beveled angle on the bridge bottom that was adapted to the bridge's size. The bevels for smaller and larger bridges were 40° and 50°, respectively. Figure 3 presents the structure of the extrusion die bridge designed in this study. Larger bridges experience higher pressures; this larger angle ensures that the upper bridge sections have both adequate strength and controlled deformation. This bridge geometry was intended to facilitate smooth material flow and simplify welding. The welding chamber was designed to balance optimal flow dynamics with adequate welding pressure. The chamber height varied from 20 mm near the center to 25 mm toward the periphery; these were selected in accordance with empirical knowledge for achieving robust welds with 7-inch

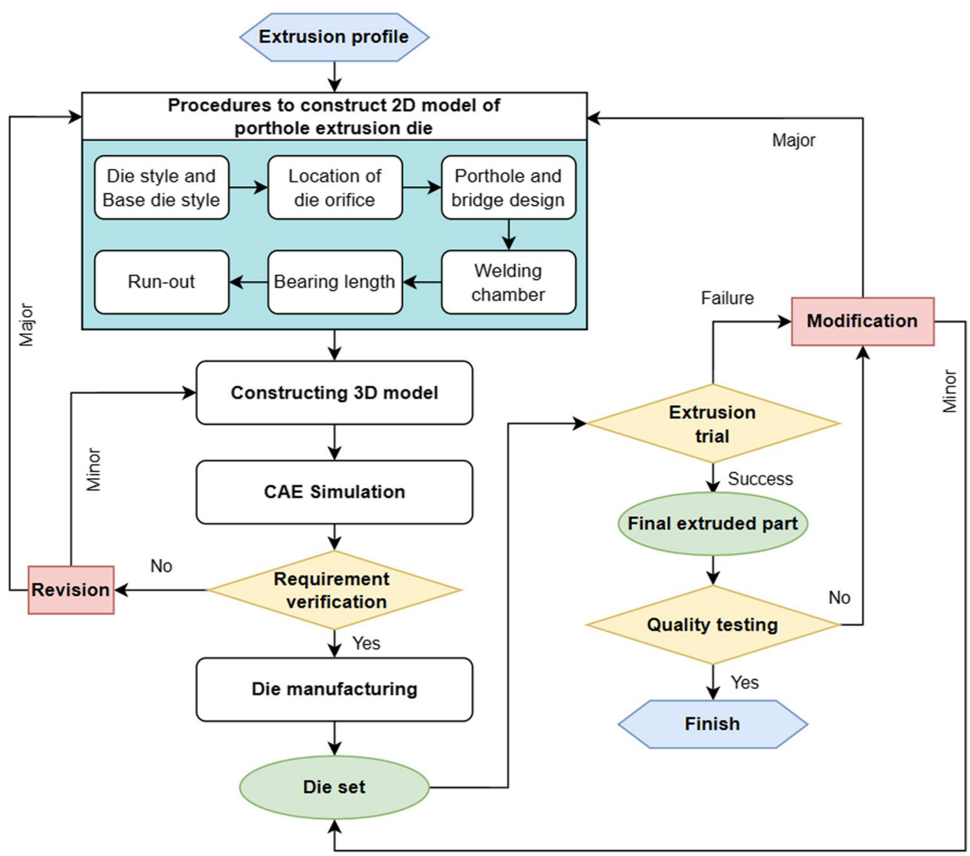


**Fig. 2** Flow chart of porthole die design process

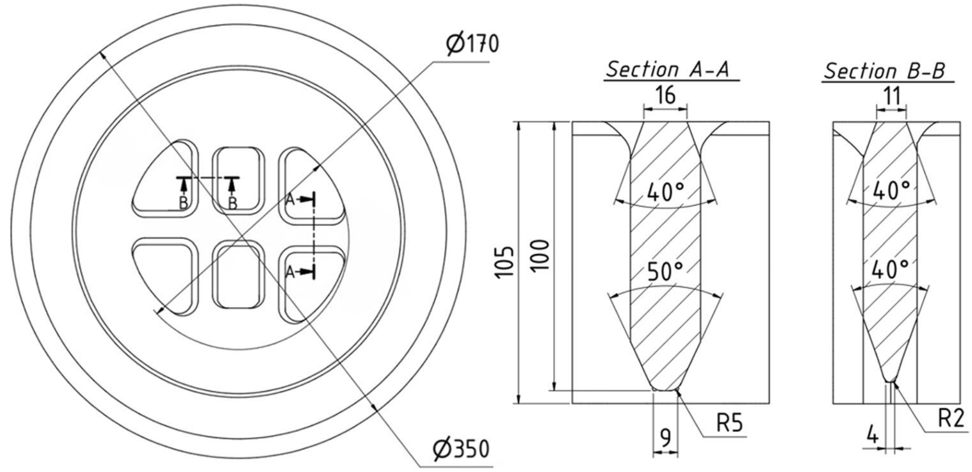


**Fig. 3** Structure of extrusion die bridge designed in the present study

billets [15, 19]. Additionally, the maximum taper angle of the chamber was 5.7° in the extrusion direction to increase its volume and, consequently, the welding pressure. This trade-off between increased welding pressure and simpler flow balancing benefited the overall die performance. Furthermore, a 3-mm-deep pocket was incorporated upstream of the die orifice to enhance flow balance and welding pressure. The pocket's offset distance was 5 mm in most locations but was increased to 9 mm near sections where the die bridge could obstruct flow (Fig. 4).

Calculating bearing length is more challenging for hollow extrusion dies than for solid extrusion dies. This complexity is attributable to the complex interplay of the product wall thickness, geometrical elements, die bridge flow resistance, porthole geometry, and the effects of dead material areas beneath the bridge. Although bearing length can be adjusted to optimize flow balance, excessive small-scale micro adjustments could compromise the surface of the extruded product. The bearing length of the initial die was primarily determined by product profile and product geometry. A simplified approach correlates bearing length to orifice width or product wall thickness using an empirically derived coefficient, $K_w$, which ranges from 1.4 to 3.5 for complex profiles and can extend to 4.5 in more complex cases [19, 20]. Hollow dies, characterized by a more complex structure than solid dies, require a modified approach. While the principles for solid dies can be applied, the obstructing effect of bridge structures necessitates shorter bearing lengths in these areas. Additionally, accelerated metal flow near the porthole center may justify longer bearing lengths in these regions. Figure 5 depicts the initial bearing length distribution across various areas of the orifice die. These lengths were further refined through simulations and actual extrusion trials. A general outline of the initial die design is shown in Fig. 6.

## 2.2 CAE modeling

Extrusion simulations were used to both design the die and monitor the process. Both steady-state and transient simulations were conducted to streamline the design verification and die refinement process for the aluminum extrusion task. Steady-state simulations were used to capture the process after material stabilization. Variables were assumed to be constant, and a fixed mesh was employed for computational efficiency. This method was effective for examining the factors affecting the die design, process parameters, and die stresses. However, transient simulations were also used to obtain a deeper understanding of the flows and potential instabilities. These simulations incorporated time-dependent behavior and a moving mesh to achieve improved observations of the process, particularly for the initial stages. Although these simulations are computationally demanding,

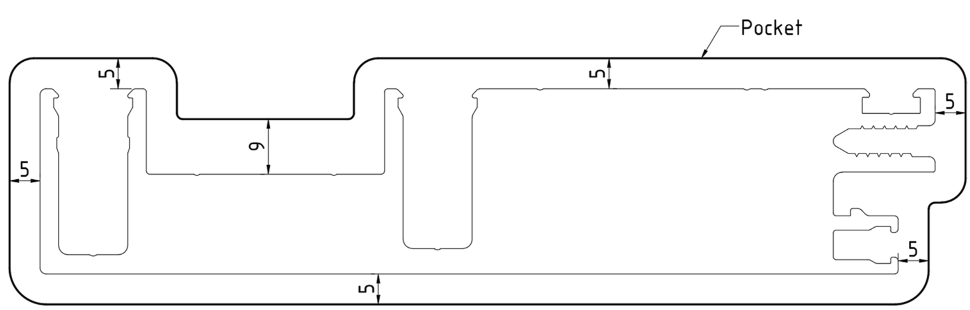


**Fig. 4** Pocket shape of initial design (unit, millimeter)

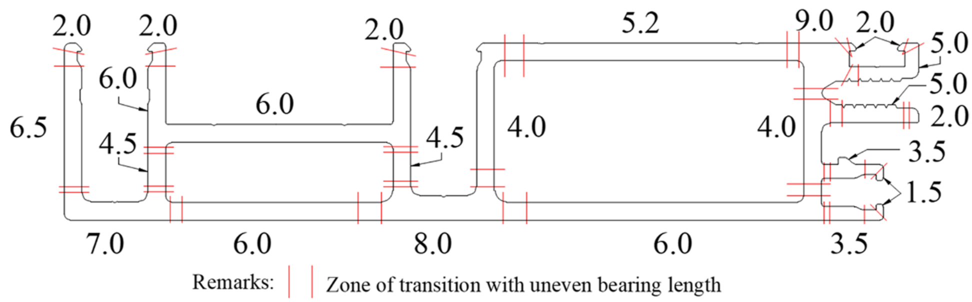


**Fig. 5** Bearing lengths of initial design (unit, millimeter)

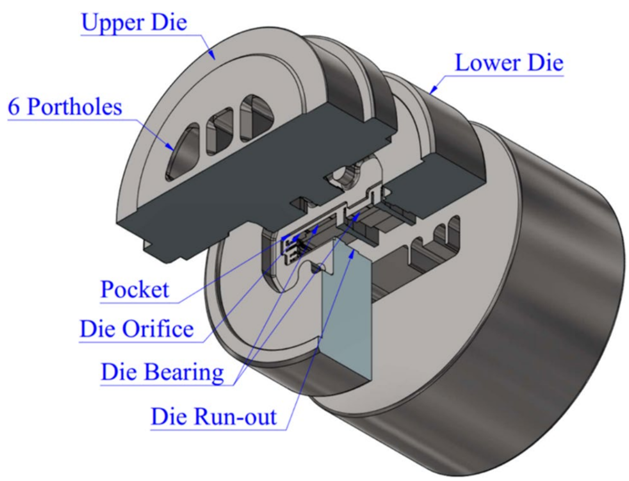


**Fig. 6** General outline of initial die design

**Table 3** Parameters of the material constitutive model

| Parameters | Values |
|---|---|
| $n$ | 5.8 |
| $A$ | $1.46 \times 10^{11}$ |
| Strain rate offset ($s^{-1}$) | 0.01 |
| $Q$ (J/mol) | $1.479 \times 10^{5}$ |
| $\alpha$ ($Pa^{-1}$) | $1.85 \times 10^{-8}$ |
| $R$ (J/mol-K) | 8.314 |

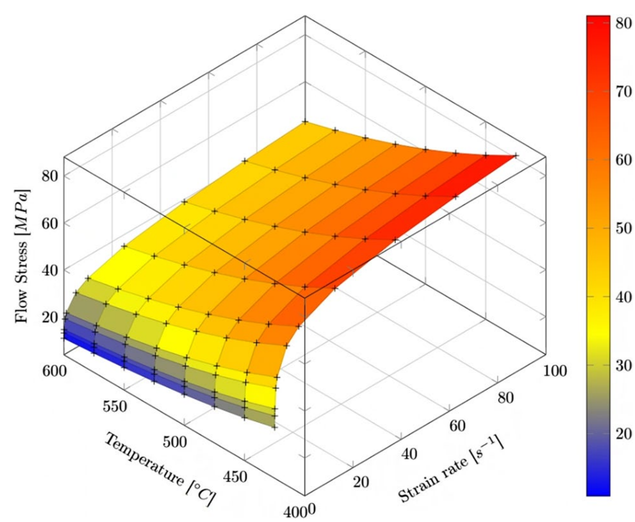


**Fig. 7** Flow stress [$\sigma = f(\dot{\varepsilon}, T)$] data for AA7005

they were highly effective for analyzing the flow and behavior of materials. Inspire Extrude Metal is a finite element analysis software designed for simulating metal and polymer extrusion processes. Developed by Altair, it utilizes the HyperXtrude solver to predict material flow, stress, velocity, temperature distribution, and welding characteristics. Additionally, the software calculates die stress by interpolating forces from the extrusion simulation onto the assembled die tooling.

An inverse hyperbolic sine model was adopted to describe the material's constitutive behavior, as expressed in (2):

$$\sigma = \frac{1}{\alpha}\sinh^{-1}[(\frac{\dot{\varepsilon} \times e^{Q/RT}}{A})^{\frac{1}{n}}] \tag{2}$$

where $\sigma$ represents the flow stress of the material; $\alpha$ is the reciprocal stress factor; $A$ is the reciprocal strain rate factor; $\dot{\varepsilon}$ is the effective strain rate; and $n$ is the stress exponent. Furthermore, the model also includes the activation energy of deformation $Q$, the universal gas constant $R$, and the absolute temperature, $T$.

Table 3 and Fig. 7 detail the material parameters of the constitutive equation and flow stress data for the selected extrusion material. A viscoplastic friction model with a coefficient of 0.3 is applied in the simulation. Table 4 presents the extrusion parameters, including the contour length, total area of the profile, and initial temperatures for the billet, die, and tools. The authors conducted the simulations utilizing Asus Pro E500 G6 workstation, ensuring computational efficiency and stability.

The initial die scheme for the porthole extrusion process was simulated as a steady-state analysis for a CAE model constructed in Altair Inspire Extrude. Meshes were generated using STEP-formatted data. To accurately represent metal flow through the extrusion tools, the model was divided into five regions for steady-state analysis (Fig. 8).

**Table 4** Extrusion simulation conditions

| Profile data | | | | Process conditions | | |
|---|---|---|---|---|---|---|
| Contour length (mm) | Area ($mm^2$) | Extrusion ratio | Billet preheat (°C) | Container temperature (°C) | Die temperature (°C) | Viscoplastic friction coefficient |
| 824.93 | 1266 | 20.75 | 460 | 430 | 460 | 0.3 |

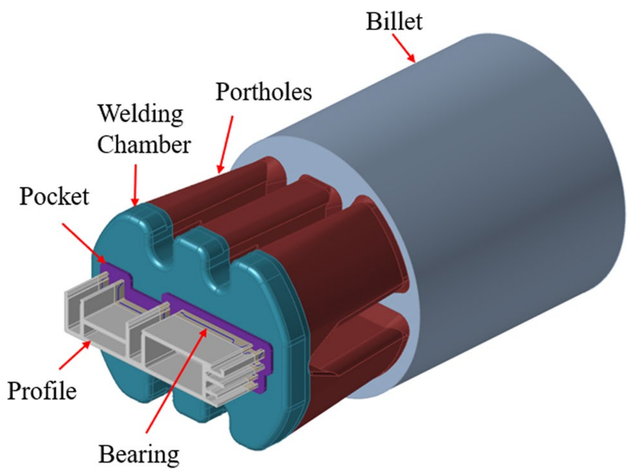


**Fig. 8** Simulation model for the porthole die extrusion process

Different element types and sizes were assigned in accordance with the anticipated magnitude of local deformation in each region and component to optimize the computational efficiency and model accuracy. The steady-state simulation model had approximately 1,300,000 elements; approximately 80% were tetrahedral elements, and the remainder were triangular prism elements.

## 3 Initial design simulation analysis

### 3.1 Die stress results

The initial die design was established on the basis of fundamental die design principles. However, the runout section was carefully designed to avoid compromising die strength and product quality during extrusion. The medium–high-strength aluminum alloys of this research require high die strength, and in the initial design, excessive stress concentrations reaching 1886 MPa at the die orifice were observed (Fig. 9a).

Therefore, the die strength was improved by implementing a sloped-down runout design after the bearing length, which significantly improved stress distribution within the die cavity, as observed in Fig. 9b. The results showed that the modified lower die improved the stress concentration at the corner positions, ensuring that no position had a stress concentration exceeding 1300 MPa.

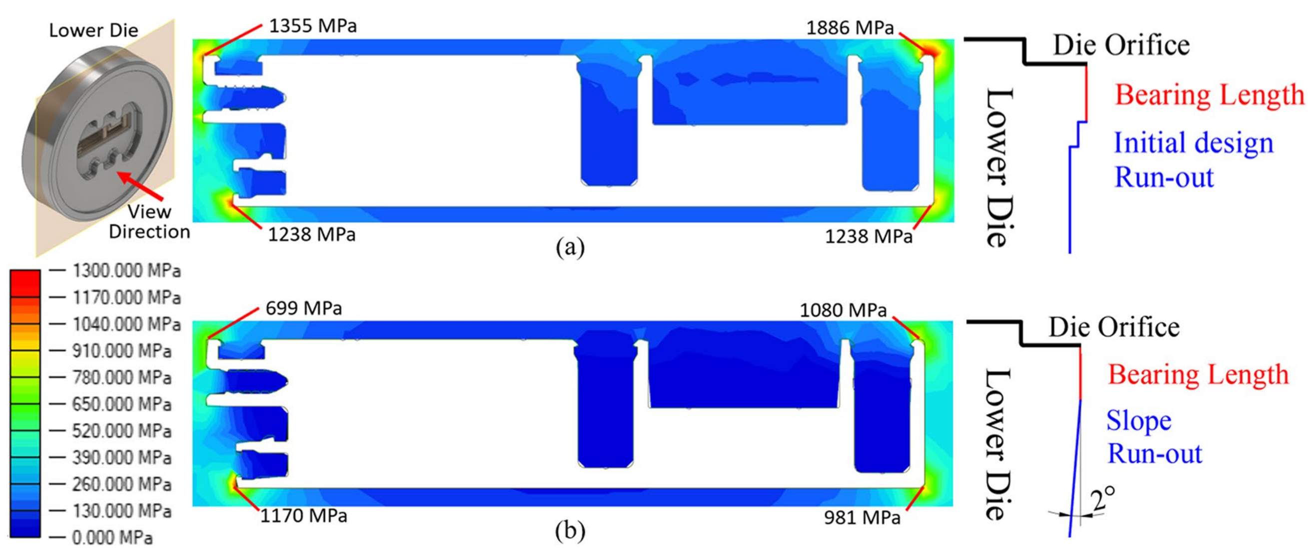


**Fig. 9** Steady-state die stress simulation results at a ram speed of 0.4 mm/s: **a** initial design runout, **b** slope runout

### 3.2 Simulation results of initial die design

Achieving uniform material flow behavior is crucial for die design, and it is frequently evaluated by analyzing the flow velocity distribution on the die exit cross-section.

When analyzing the flow behavior of the porthole extrusion die, the velocity distribution at the die exit is a crucial indicator of uniform billet flow. Initial simulations at a ram speed of 0.4 mm/s (Fig. 10) revealed a range of velocities between 8.07 and 8.76 mm/s. Unlike typical dies for which material concentrates toward the center because of frictional resistance, the varying volumes of the six portholes of this design affect the amount of material directed into the welding chamber by each porthole.

As depicted in Fig. 11, the weld lines generated by portholes 3 and 4 lie entirely within Region A, which exhibits the highest simulated extrusion velocities. Here, the flow combination effectively accumulates kinetic energy prior to passing through the die orifice. A similar phenomenon occurs with the weld seam between portholes 1 and 2, but its location near the center of the die experiences less flow resistance, resulting in lower energy accumulation compared to Region A. Furthermore, porthole 2 in Region B is intentionally designed with a 25% smaller volume than the peripheral portholes. This aims to reduce the amount of

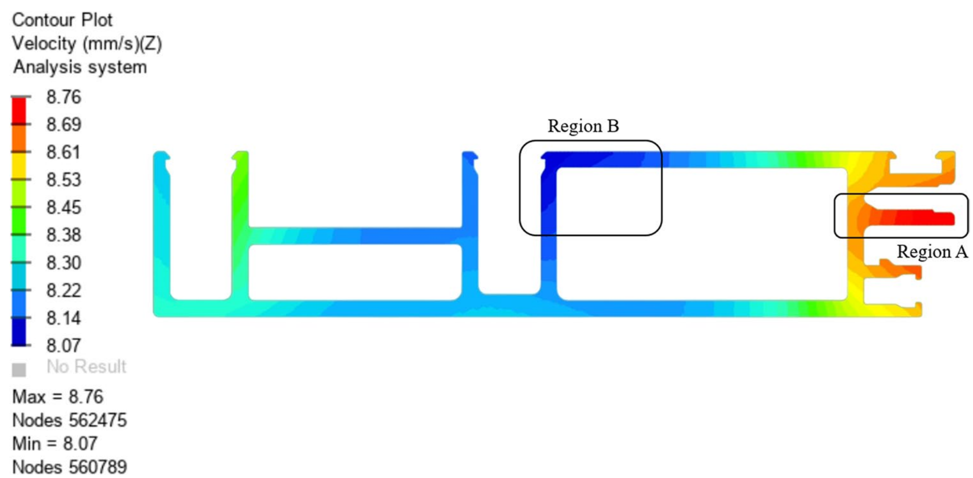


**Fig. 10** Velocity distribution on the cross-section of die exit for initial die design at a ram speed of 0.4 mm/s

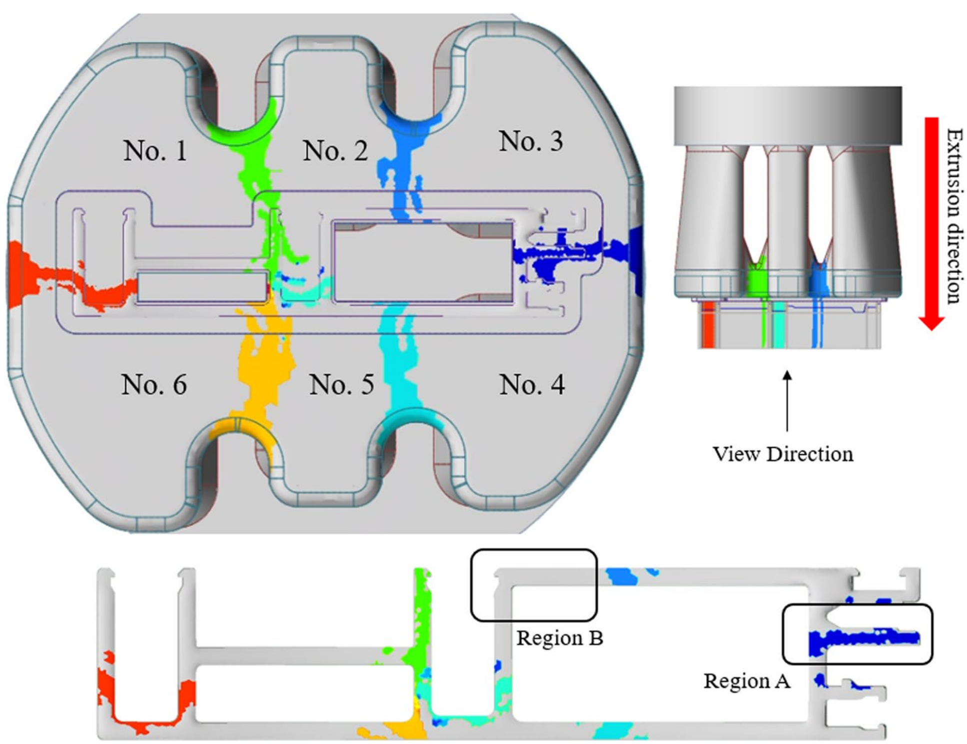


**Fig. 11** Location of portholes and simulation results of weld seams at ram speed 0.4 mm/s

material fed into the center and mitigate the typical center-focused velocity distribution observed in conventional designs. The effectiveness of this strategy is evident in the simulated results, showing the lowest flow velocity distribution at the die exit in Region B.

## 4 Die trials

The die design was refined iteratively through a loop of CAE analysis, result evaluation, and subsequent design modifications. These modifications, such as changing the runout in the lower die, significantly improved the die strength. The improved design was then manufactured for experimental trials. Figure 12 presents the manufactured die set for the initial die design, including the upper die, lower die, and backer.

### 4.1 First die trial

The study targeted the extrusion of a specific product profile using a porthole die on a 7-inch billet, 2100-ton press. Initial extrusion experiments at speeds of 0.1 and 0.4 mm/s with 7000-series medium–high-strength aluminum alloy revealed significant challenges. Accordingly, corresponding simulations were performed. The simulation at 0.1 mm/s was used to compare the initial extrusion stages with the real extrusion front end. Furthermore, the simulation at 0.4 mm/s was employed to evaluate extrusion force during the stable extrusion phase, which experimentally occurs at this velocity. All simulations were conducted under the temperature conditions outlined in Table 4, mirroring the actual extrusion process. Figure 13 indicates the front end of the extruded product after the first attempt with the initial die set. Although most of the sections were properly formed, two crucial features were incomplete.

Although the initial design attempted to limit center-focused flow, in the actual extrusion, the opposite occurred; the material flowed faster in the middle than at the periphery. This can be attributed to the numerous small, ribbed features at the edge that generate high resistance at the die wall,

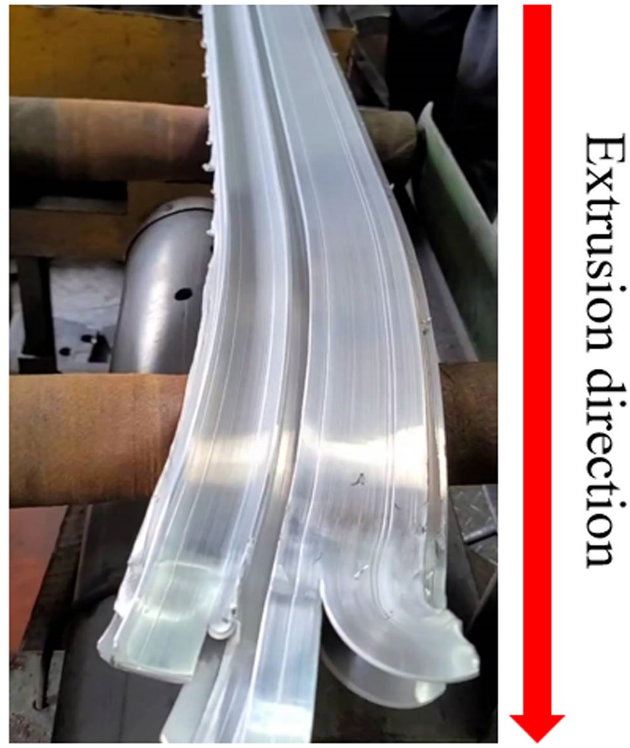


**Fig. 13** Front end of the extruded product after first extrusion test

hindering flow. Conversely, the central material encountered less resistance and was extruded faster. This differential flow caused the central material to undesirably "pull" trapped material from the periphery, leaving these areas underfilled and unformed.

The complex profile details and intricate geometry at the periphery also contribute to increased flow resistance; this is an inherent challenge of extrusion. The small gap of 1.9 mm on incomplete feature 1 results in an alarmingly thin section with compromised strength and susceptibility to tearing (Fig. 14). Incomplete feature 2, which has a slightly thinner gap (2.8 mm), has a long bearing length, which amplifies resistance and eventually leads to extrudate breakage.

The results of this first extrusion trial were crucial indicators for necessary improvements and refinements to the

**Fig. 12** Machined die set of the initial design

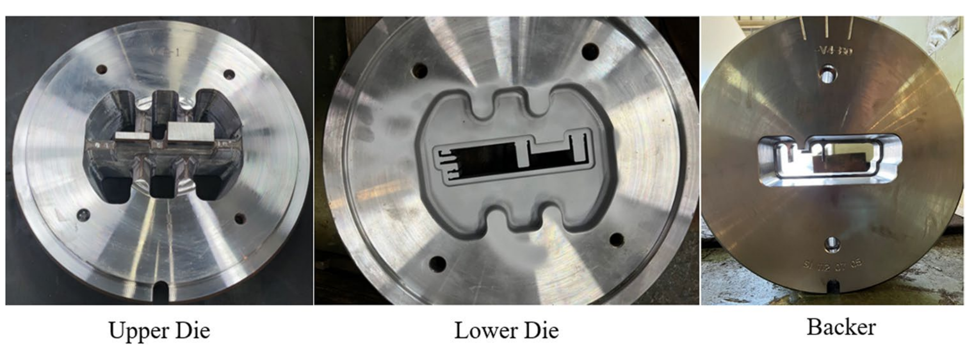

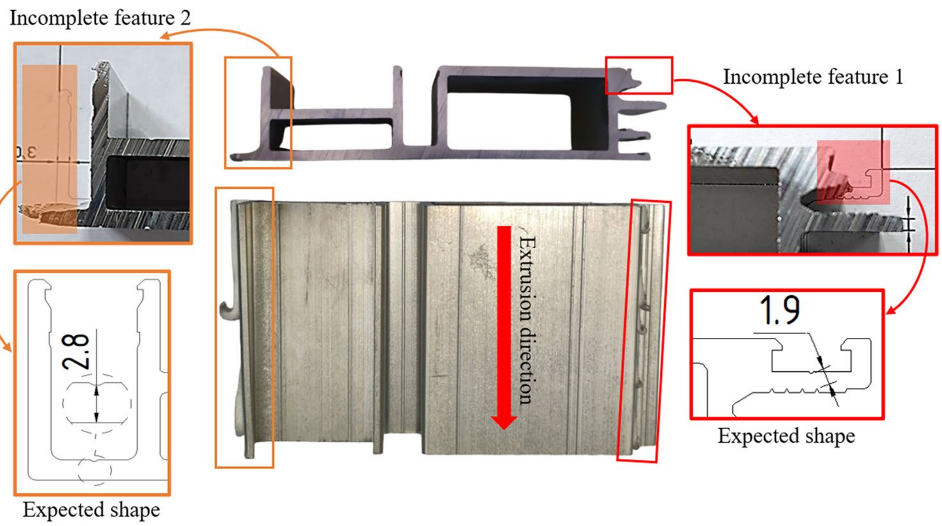


**Fig. 14** Cross-sections of extruded products and incomplete features in the first extrusion trial

initial die design; subsequent optimization efforts were based on these results.

## 4.2 Minor revision and second die trial

To overcome the deficiencies observed in the initial extrusion trial, a series of targeted modifications were implemented to enhance material flow and mitigate resistance in the problematic regions. The primary focus was adjusting the bearing lengths and expanding the die runout exit angles. As illustrated in the flowchart in Fig. 1, these modifications were executed on-site at the extrusion facility. Figure 15 provides a detailed overview of the modifications. The bearing lengths within incomplete feature 1 were reduced from 5 to approximately 3 mm, and those in incomplete feature 2 were decreased from 7 and 6.5 to 3.6 and 3.9 mm, respectively. Furthermore, offset areas with a width of approximately 1 mm were integrated in all modified regions. These adjustments collectively created a superior flow path, alleviated material blockages, and facilitated complete feature formation during extrusion.

The second extrusion trial yielded a mixture of successful and unsuccessful outcomes. Although progress in some aspects was observed, complete and successful extrusion of the entire profile cross-section was not achieved. Figure 16 depicts the front end and extruded profile obtained for this test. Incomplete feature 1 was successfully formed; this was a notable advancement. Additionally, the material flow along the right side in the extrusion direction was better balanced with the flow in the central extrusion area. However, severe material blockages were observed; in particular, the modifications implemented in the incomplete feature 2 region failed to produce the desired effects. The successful extrusion of incomplete feature 1 resulted in a smoother and faster material flow in that area, which resulted in the extrudate unexpectedly tilting toward the left (in the extrusion direction). This unintended shift intensified the collision of the material at the incomplete

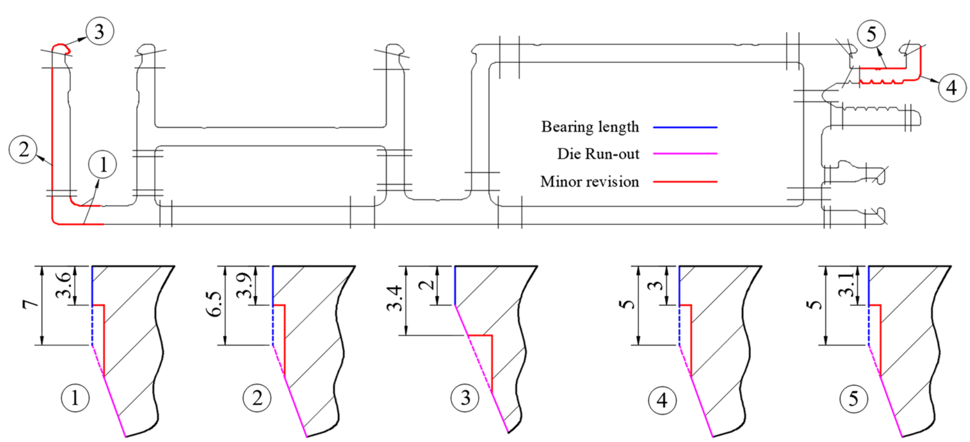


**Fig. 15** Detailed modifications in minor revision

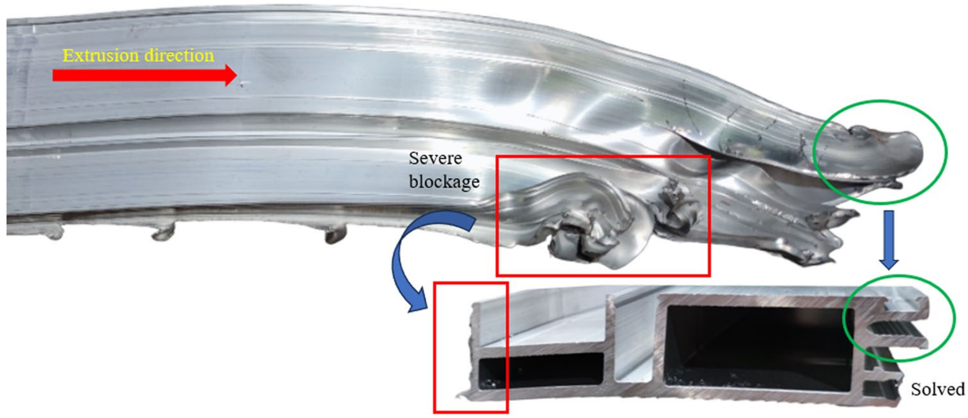


**Fig. 16** Front end and extruded profile obtained from the second extrusion trial

feature 2 with the die walls and the runout, resulting in nonuniform flow and breakage.

Furthermore, post-extrusion inspections revealed significant deformation within the lower die (Fig. 17). This damage was attributed to the severity of the material blockages experienced during the trial. Flow blockages are not uncommon in extrusion processes involving 6000-series aluminum alloys such as AA6061 or AA6063; however, they typically do not cause irreparable damage to the die. This result emphasizes the increased difficulties associated with extruding high-strength aluminum alloys.

The substantial damage sustained by the lower die necessitated its complete replacement, marking a key decision point in the research process. A major revision to the design was developed to overcome the remaining challenges to successfully extrude the entire profile cross-section. The revision is described in detail in the next section.

## 5 Major revision of die design

The initial die had an uneven flow distribution resulting in extrusion defects, such as deformation, bending, and thickness variations. Although the first and second extrusion trials provided valuable insights, neither achieved the desired outcome. Targeted and effective optimization strategies for the die structure were implemented to overcome the extrusion challenges.

### 5.1 Bearing length optimization

Bearing length optimization is a critical part of the extrusion die design process that is typically undertaken at the final stage following a thorough analysis and evaluation of the initial design. The bearing length is a definitive control point that ensures that the material consistently flows through the die orifice at the desired velocity. The arrangement of the bearing lengths directly influences the quality of the final extruded product.

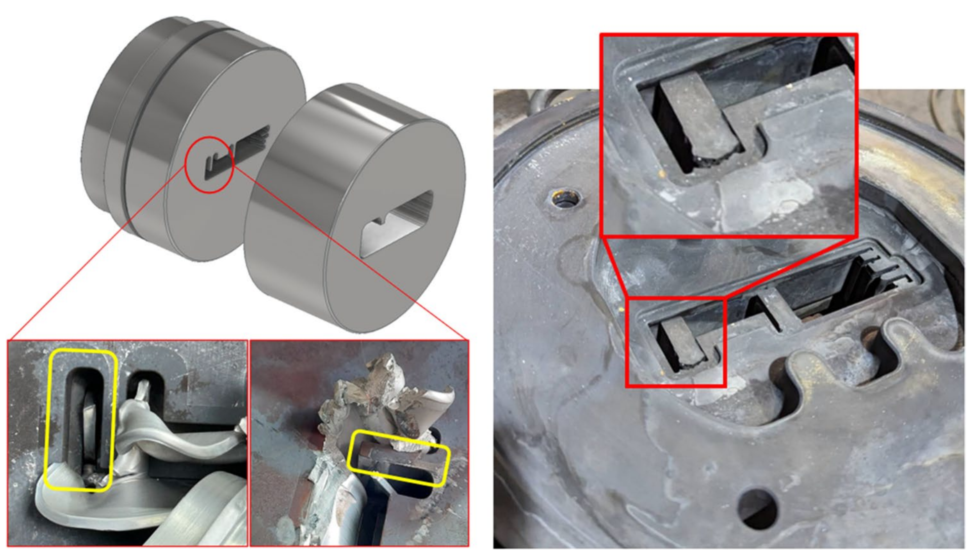

**Fig. 17** Severe blockage and irreparable damage of the lower die

The experimental results in the initial design phase were used to guide a series of modifications for resolving incomplete feature formation in the extruded profile. Minimizing friction in these problematic regions was the primary objective. This was achieved by reducing the bearing lengths within specific areas of the die. Figure 18a presents the key bearing length locations.

The largest adjustments were performed in areas 21 and 22. The bearing length in area 21 was reduced by more than 40% and repositioned toward the corner of the profile. The taper transitions between areas 17, 20, and 21 were modified; a similar adjustment was applied between areas 21 and 23. These collective alterations eliminated equal bearing lengths within area 22. Figure 18b presents the final bearing length parameters after modification.

## 5.2 Adjusting die runout

The initial design and subsequent modifications of the extrusion die prioritized maximizing die strength because of the difficulty of extruding the chosen alloy. For example, the steep-runout sections immediately following the bearing length effectively increased the lower die's strength, as discussed in Section 3.1. However, upon further analysis of the experimental results, a more nuanced approach to die runout design was adopted. Instead of focusing on maximizing strength, the extrudate can be guided after shaping at the die orifice by modifying the runouts. This prevents the accumulation of molten metal within the die cavity, ensuring a smooth and defect-free process. The subsequent design adjustments were intended to achieve successful extrusion of the entire profile while meeting the desired technical specifications.

The shortcomings of the initial steep-runout design were revealed in a simulation (Fig. 19a). The small taper angle led to prolonged contact between the profile and the runout die after exiting the orifice, significantly increasing resistance and hindering material flow. To overcome this, an offset area of approximately 0.5 mm was introduced after the bearing length, providing additional clearance for the extrudate and minimizing collision with the runout. Furthermore, the slope angle was adjusted to a range of 5°–7°, replacing the steep 2° angle. Figure 19b depicts the simulation results for these modifications; the flow behavior has clearly improved. Figure 20 presents the design changes implemented in the machined die.

## 5.3 Modifying the shape and dimensions of the die pocket

The extrusion trials revealed the limitations of the initial pocket design in the lower die. Therefore, an adaptively shaped pocket was implemented to enhance flow stability, reduce dead zones, and improve die filling when extruding the complex profile [9, 15, 16]. Approaches for modifying the shape of the pocket when adjusting the die have been investigated in numerous studies. These modifications are especially effective for affecting flow behavior and extrusion force.

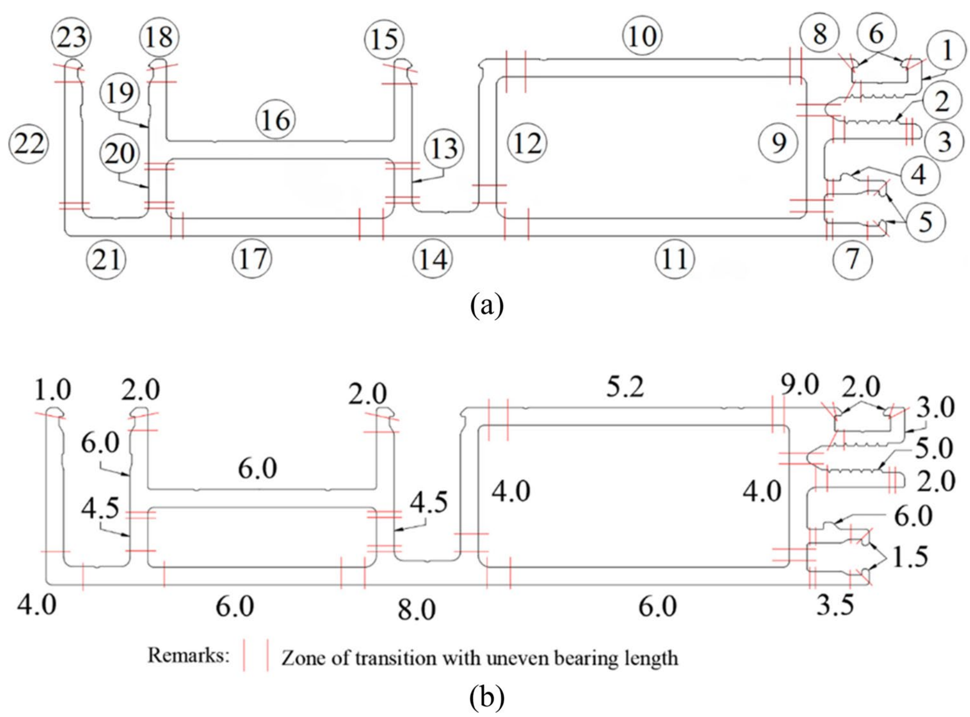


**Fig. 18** Bearing lengths: **a** marked positions and **b** major revision of bearing length

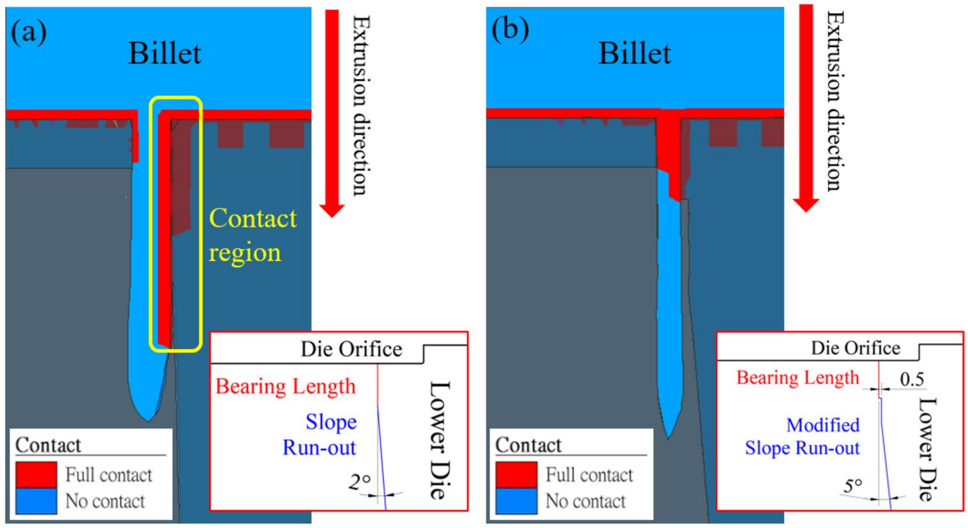


**Fig. 19** Runout contact simulation results of **a** initial design and **b** major revision

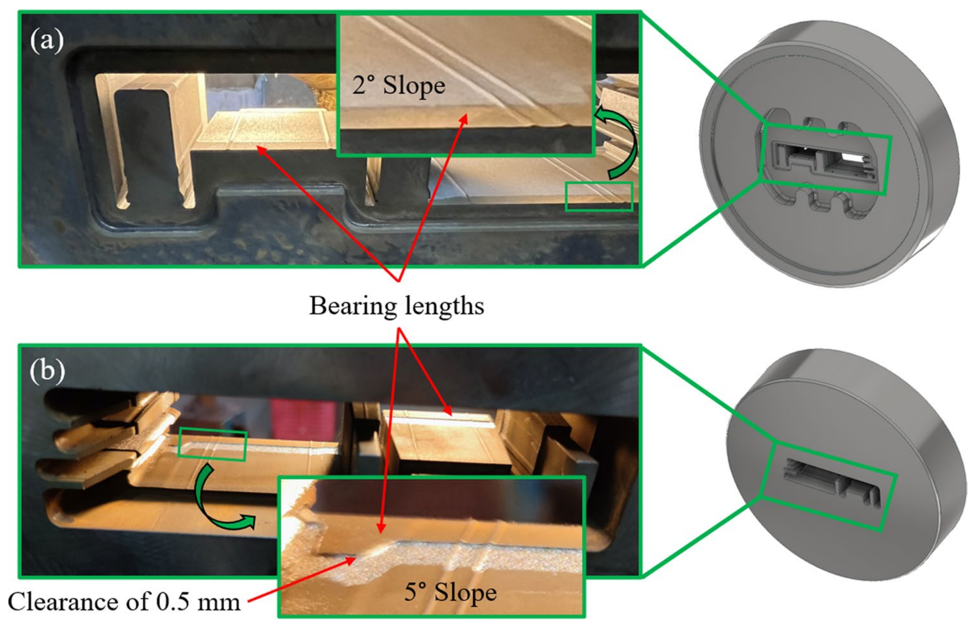


**Fig. 20** Design changes implemented in machined die: **a** before and **b** after modification

The initial pocket profile was established by offsetting the outer positions of the extruded profile by 5 mm, forming the base for subsequent adaptations. Subsequently, the pocket design was modified in accordance with specific regions and their characteristics. Figure 21 presents a comparison of the original and modified pocket profiles, highlighting the target modifications for incomplete feature 2. Here, the pocket was expanded from 5 to 8 mm to direct more material into this area and handle potential flow problems. Conversely, observations from previous extrusions revealed that the flow was faster in the central region than in the periphery. To overcome this uneven flow distribution, the pocket profile in this area was decreased by 1.7 mm.

These specific modifications are examples of the advantages of an adaptive pocket design for optimizing the material distribution and flow within the die cavity. This approach is promising for improving the overall profile formation and extrusion quality, particularly for complex profiles.

The simulation results for the velocity distribution at the cross-section of incomplete feature 2 are shown in Fig. 22a. In the highlighted area, the distribution is markedly uneven, suggesting that the inappropriate pocket profile hindered material inflow, contributing to the severe blockage encountered during the second extrusion test with the initial die design. By contrast, the flow pattern is greatly improved in the modified design with the proposed adaptive-shape pocket design. This improvement in the distribution demonstrates the potential of this adaptive approach to handle flow imbalances and to improve the overall die design performance.

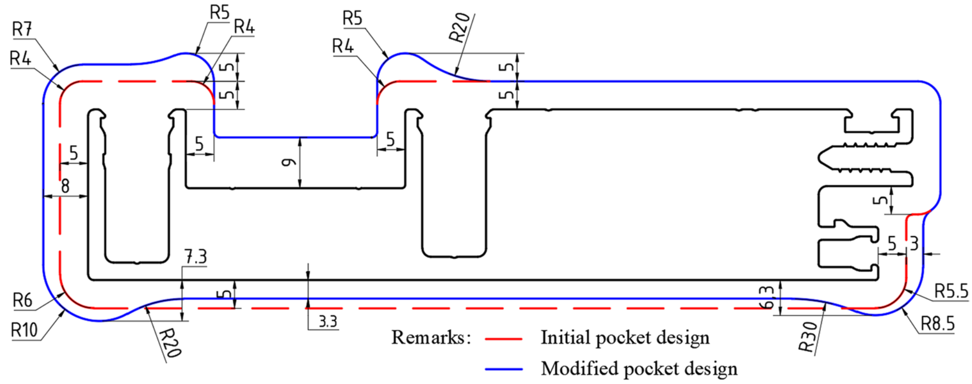


**Fig. 21** Comparison of original and modified pocket profiles

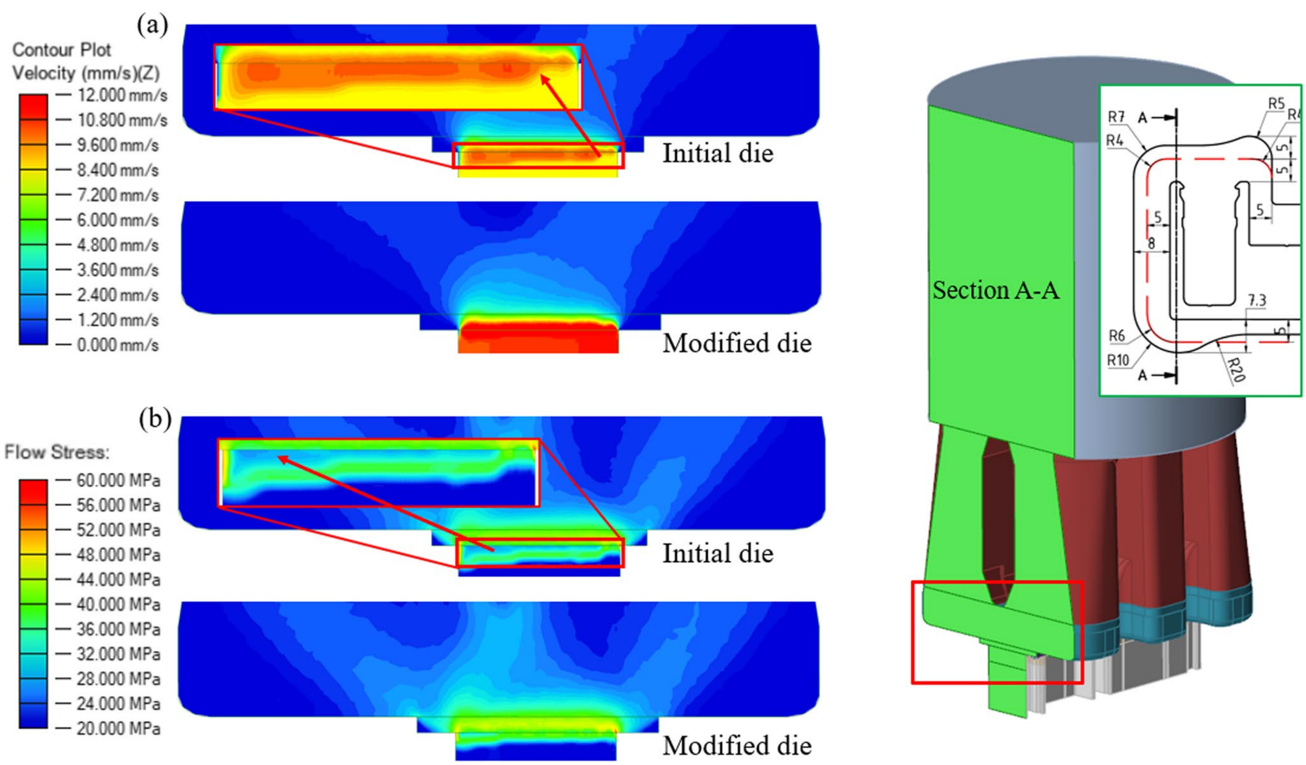


**Fig. 22** Simulation results (ram speed of 0.4 mm/s) for the initial die and modified design at the cross-section of incomplete feature 2: **a** z-direction velocity distribution and **b** flow stress distribution

A weld seam in the region of incomplete feature 2 is visible in Fig. 11. Welding has not yet occurred in this area, which is considered an aspect of preventing profile shaping. Figure 22b presents a disturbance in the flow stress distribution at the die orifice of the initial design; this disturbance seems to affect the welding process in this location. After modifying the shape of the pocket, the flow stress decreases substantially at the mentioned location, facilitating the establishment of the welding process and avoiding breaks between material flows that might result in unsuccessful shaping.

Major revisions were implemented for the bearing length, die runout, and pocket shape, resulting in an enhanced design. Figure 23 presents the simulated velocity distribution at the extrusion exit section for this enhanced design. The material flow was greatly improved at incomplete feature 2. Compared with the initial design, the velocity in the *z*-direction within the region increased by 2.23 to 2.70 mm/s, a notable enhancement. The velocity of the flow at the welding seam also increased from 8.14 to 10.60 mm/s, further demonstrating the effectiveness of the proposed design.

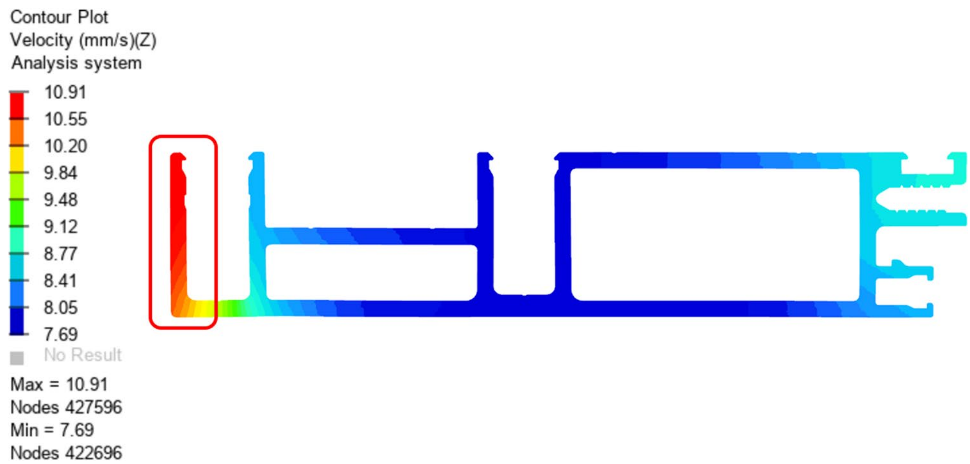


**Fig. 23** Velocity distribution at extrusion exit section of the major revision die with a ram speed of 0.4 mm/s

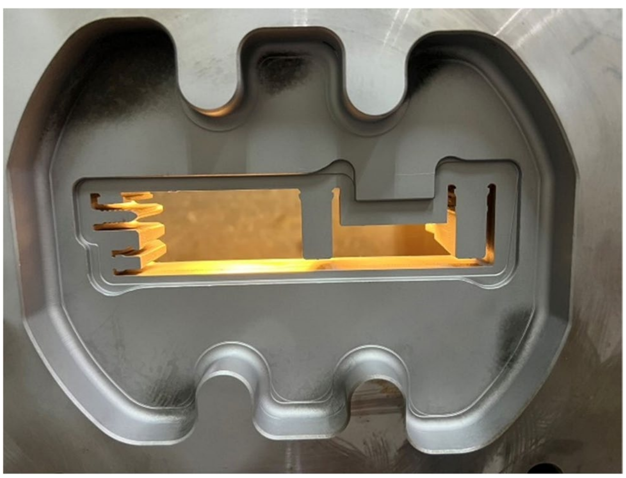

**Fig. 24** Lower die for the major revision design

## 6 Extrusion experiment validation

In accordance with the major design revision, an alternative lower die was machined. Figure 24 presents the completed lower die, showcasing the implemented modifications. Validation extrusion experiments were then conducted to evaluate the performance of this enhanced design.

### 6.1 Final extruded product

The validation experiments yielded highly encouraging outcomes, culminating in the successful extrusion of the entire complex profile, as depicted in Fig. 25a. Initially, the extrusion speed was set at 0.1 mm/s to observe and verify successful extrusion. Then, the simulation results at 0.1 mm/s were compared to the actual front-end extrusion results. The changes in material flow velocity between the periphery and central regions (clearly observable at the extrusion front end in Fig. 25b) were consistent with the predictions of the proposed simulation model (Fig. 25c). This emphasizes the importance of ensuring unobstructed material flow throughout the extrusion process when designing dies for complex profiles and high-strength aluminum alloys.

To assess product quality, dimensional measurements were performed on the extruded product following each trial. The dimensions that were measured are depicted in Fig. 26, and the measurement results are given in Table 5. Overall, the attained dimensions demonstrate the die's suitability for real-world applications. Notably, the revisions improved most profile dimensions; dimensions C and M were particularly superior. Thus, the final product was more refined.

### 6.2 Peak extrusion force

Extrusion force is a key parameter for optimizing extrusion processes, determining capacity, and designing tools. Table 6 presents the maximum extrusion forces recorded during actual extrusion trials for both the initial and final modified dies along with the corresponding simulation results. During extrusion experiments, force data was continuously collected as the pressure within the main and the support cylinder. These data were subsequently converted to force units by using (3):

$$F = \left(\frac{\pi \times D^2}{4} + 2 \times \frac{\pi \times d^2}{4}\right) \times \mathrm{P} \tag{3}$$

where $D$ denotes the diameter of the main cylinder of the hydrostatic press machine (1000 mm in this case), $d$ is the diameter of the support cylinder (220 mm in this case), and $P$ is the collected pressure, measured in kg/cm$^2$.

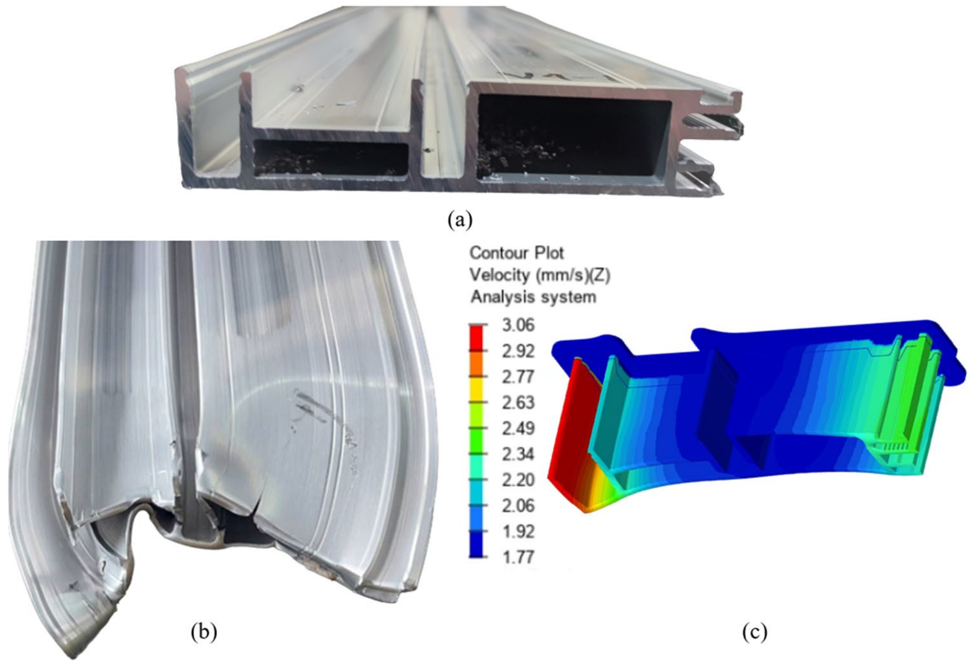


**Fig. 25** Experimental extrusion profile. **a** Final product. **b** Real front end. **c** Simulation front end (at ram speed 0.1 mm/s)

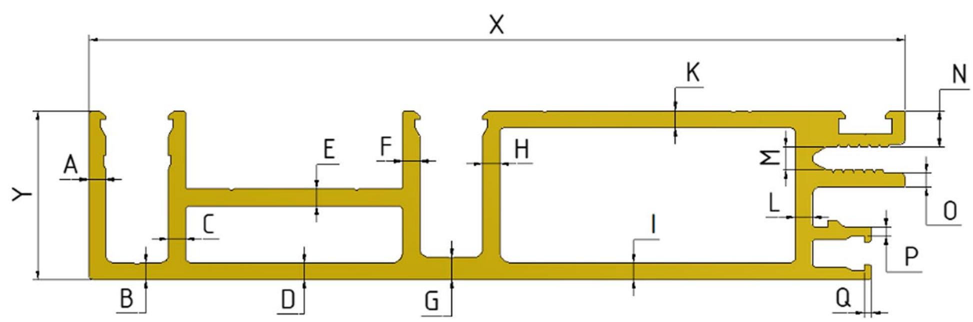


**Fig. 26** Dimensions of extrusion product

The analysis shows the difference between the actual and predicted forces, especially for the original die. This difference is likely due to material becoming stuck in the die, which creates resistance and increases the force needed for extrusion. The initial die had a 19.7% difference in force at a speed of 0.1 mm/s. This large difference suggests that material flow was blocked in the die, leading to higher pressure and force. However, the modified die had a very small difference of less than 1% at the same speed, indicating smoother material flow. Although the simulation results indicated that the extrusion force varied little between the designs, real-world trials revealed a noteworthy 7.4% reduction in the final modified design compared with the initial design (1300 vs. 1404 tons) at a ram speed of 0.4 mm/s. The revised die design effectively addressed the flow problems in the initial die, which decreased the friction in problematic areas and decreased the overall force required for extrusion.

## 7 Conclusions

A porthole extrusion process was designed for a complicated profile of AA7005, a medium–high-strength aluminum alloy. CAE simulations were employed to analyze die strength and predict material flow balance across the front-end profile section at the die exit. Initial practical evaluations through extrusion experiments revealed that some features within the profile were not extruded successfully with the initial die design. Subsequently, a minor revision was implemented directly on the machined die, somewhat improving the results but not attaining complete success. A severe material blockage damaged the initial die, necessitating a comprehensive revision of the design approach. Drawing upon insights gained from the previous experimental results and leveraging CAE simulations, a major revision was undertaken that encompassed

**Table 5** Dimensions of the extrusion product in extrusion tests

| Dimension | Nominal value | Initial design (first extrusion test) | Minor revision (second extrusion test) | Major revision (validation test) |
|---|---|---|---|---|
| X | 145.00 | - | - | 145.32 |
| Y | 30.00 | 30.19 | 30.17 | 30.16 |
| A | 3.00 | - | - | 3.05 |
| B | 3.00 | - | - | 3.05 |
| C | 3.00 | 2.75 | 2.75 | 3.02 |
| D | 3.00 | 3.10 | 3.02 | 3.02 |
| E | 3.00 | 3.02 | 2.98 | 3.02 |
| F | 3.00 | 3.02 | 2.99 | 2.98 |
| G | 4.00 | 4.09 | 4.05 | 4.07 |
| H | 3.00 | 3.07 | 3.02 | 3.00 |
| I | 3.00 | 3.03 | 2.92 | 2.98 |
| K | 3.00 | 3.05 | 3.02 | 3.01 |
| L | 3.00 | 2.92 | 2.86 | 3.03 |
| M | 4.00 | - | 3.95 | 3.98 |
| N | 6.00 | - | 6.05 | 6.03 |
| O | 2.50 | 2.50 | 2.48 | 2.50 |
| P | 1.70 | 1.70 | 1.70 | 1.71 |
| Q | 1.20 | 1.25 | 1.24 | 1.21 |

Unit, millimeter

**Table 6** Simulation and experimental extrusion force results

| Version | Ram speed | Cylinder pressure | Experiment force | Simulation force | Difference |
|---|---|---|---|---|---|
| | (mm/s) | (kg/cm$^2$) | (tons) | (tons) | (%) |
| Initial die | 0.1 | 140 | 1205 | 967 | 19.7 |
| | 0.4 | 163 | 1404 | 1278 | 8.9 |
| Revised die | 0.1 | 118 | 1016 | 981 | 3.5 |
| | 0.4 | 151 | 1300 | 1296 | $< 1$ |

adjustments to bearing length, die runout, and pocket shape. A validation extrusion test was then conducted to assess the effectiveness of the implemented modifications. The conclusions are as follows:

- A detailed account of the porthole extrusion die design process for a complex profile fabricated from the medium–high-strength aluminum alloy was provided. Using the curtain structure as an example of the complex profile, the study successfully applied AA7005 to extrude this desired product. The proposed design successfully achieved complete extrusion of the targeted profile using only the base die material.
- The initial design of the pocket resulted in uneven velocity distributions at incomplete features. After modification, the flow patterns were improved, demonstrating the potential of an adaptive-shaped pocket design to handle flow imbalances and enhance die design performance. The design also improved *z*-direction velocity and flow stress distribution, facilitating welding and avoiding material flow breaks. Moreover, the die design with sloped walls for die runout was effective for improving die strength without hindering extrusion flow.
- The final revised die set was highly promising in terms of the product dimensions. All of the measured dimensions of the extruded profile met the criteria for real-world applications, demonstrating the efficacy of the implemented design modifications. Furthermore, a notable reduction in the required extrusion force (up to 7.4% compared with the initial design) was observed.

The process presented in this study not only facilitated the successful extrusion of a challenging profile but also represented a valuable roadmap for future research in high-strength aluminum alloy extrusion. The combination of simulation techniques, iterative design refinements, and experimental validation offers a framework for tackling complexities in this field and paves the way for further advancements in extrusion technology.

**Acknowledgements** The authors would like to acknowledge The Industrial Bureau of the Ministry of Economic Affairs, Taiwan, for providing partial financial support, and Goodcomer Co., Ltd. for the assistance with porthole die extrusion experiments.

**Author contribution** Thanh-Cong Nguyen: synthesized data, and writing—original draft, visualization, simulation, review, and editing; Tat-Tai Truong: designed the initial dies, reviewed and edited the content; Jun-Wei Wang: investigation, simulation; Jinn-Jong Sheu: reviewed and edited the manuscript; Chih-Lin Hsu: funding acquisition, resources, reviewed the manuscript; Quang-Cherng Hsu: funding acquisition, methodology, instructed, supervised, reviewed, and edited the manuscript.

**Funding** This research was partially funded by the Industrial Bureau of the Ministry of Economic Affairs, Taiwan, under the grant project entitled Entrusting the die and mold manufacturing application transformation and upgrading—Optimizing industrial manufacturing (high T/D ratio curtain structure aluminum extrusion profile project).

## Declarations

**Conflict of interest** The authors declare no competing interests.

## References

1. Saha PK (2000) Aluminum extrusion technology. ASM International
2. Bauser M, Siegert K (2006) Extrusion. ASM International
3. Aluminum Extruders Council (2013) Aluminum extrusion manual, 4th edn. https://aec.org/aluminum-extrusion-manual. Accessed 7 Feb 2024
4. Sheppard T (2013) Extrusion of aluminium alloys. Springer Science & Business Media
5. Mazzolani FM, Formisano A (2024) Concept, design and construction of an aluminium alloy housing prototype in seismic zone. International Conference on the Behaviour of Steel Structures in Seismic Areas. pp 855–862. https://doi.org/10.1007/978-3-031-62888-7_74
6. You X, Xing Z, Jiang S et al (2024) A review of research on aluminum alloy materials in structural engineering. Dev Built Environ: 100319. https://doi.org/10.1016/j.dibe.2023.100319
7. Al-Alimi S, Yusuf NK, Ghaleb AM et al (2024) Recycling aluminium for sustainable development: a review of different processing technologies in green manufacturing. Results Eng: 102566. https://doi.org/10.1016/j.rineng.2024.102566
8. Memari AM (2013) Curtain wall systems: a primer. American Society of Civil Engineers. https://doi.org/10.1061/9780784412701
9. Zhao H, Wang HN, Wang MJ, Li GY (2012) Simulation of extrusion process of complicated aluminium profile and die trial. Trans Nonferrous Met Soc China 22(7):1732–1737. https://doi.org/10.1016/S1003-6326(11)61380-0
10. Jie Y, Liu ZW, Zeng WQ (2021) Isothermal extrusion speed curve design for porthole die of hollow aluminium profile based on PID algorithm and finite element simulations. Trans Nonferrous Met Soc China 31(7):1939–1950. https://doi.org/10.1016/S1003-6326(21)65628-5
11. Bressan JD, Martins MM, Button ST (2015) Analysis of aluminium hot extrusion by finite volume method. Mater Today: Proc 2(10):4740–4747. https://doi.org/10.1016/j.jmatprotec.2007.12.084
12. Wang D, Zhang C, Wang C, Zhao G, Chen L, Sun W (2018) Application and analysis of spread die and flat container in the extrusion of a large-size, hollow, and flat-wide aluminum alloy profile. Int J Adv Manuf Technol 94:4247–4263. https://doi.org/10.1007/s00170-017-1127-y
13. Qian D, Li G, Deng J, Wang F (2020) Effect of die structure on extrusion forming of thin-walled component with I-type longitudinal ribs. Int J Adv Manuf Technol 108:1959–1971. https://doi.org/10.1007/s00170-020-05490-9
14. Wang X, Sun K, Liu Z, Li L, Li S, Li F (2021) A novel protection-type porthole die for manufacturing multi-cavity and thin-walled extrusion profile: numerical simulation, optimization design, and experimental validation. Int J Adv Manuf Technol 116(5):1691–1706. https://doi.org/10.1007/s00170-021-07582-6
15. Ji H, Qiao J, Kang N, Wang X, Huang J (2023) Optimization of hot extrusion process parameters for 7075 aluminum alloy rims based on HyperXtrude. J Market Res Technol 25:4913–4928. https://doi.org/10.1016/j.jmrt.2023.06.239
16. Liu Z, Li L, Li S, Yi J, Wang G (2018) Simulation analysis of porthole die extrusion process and die structure modifications for an aluminum profile with high length–width ratio and small cavity. Materials 11(9):1517. https://doi.org/10.3390/ma11091517
17. Liu Z, Li L, Wang G, Yi J (2020) Analysis and improvement of material flow during extrusion process using spreading pocket die for large-size, flat-wide, and multi-ribs profile. Int J Adv Manuf Technol 107:1115–1129. https://doi.org/10.1007/s00170-020-04971-1
18. Kathirgamanathan P, Neitzert T (2009) Optimization of pocket design to produce a thin shape complex profile. Prod Eng 3:231–241. https://doi.org/10.1007/s11740-009-0161-5
19. Truong T-T, Hsu Q-C, Tong V-C, Sheu J-J (2020) A design approach of porthole die for flow balance in extrusion of complex solid aluminum heatsink profile with large variable wall thickness. Metals 10(5):553. https://doi.org/10.3390/met10050553
20. Truong T-T, Hsu Q-C, Tong V-C (2019) Effects of solid die types in complex and large-scale aluminum profile extrusion. Appl Sci 10(1):263. https://doi.org/10.3390/app10010263
21. Hsu Q-C, Chen Y-L, Lee T-H (2014) Non-symmetric hollow extrusion of high strength 7075 aluminum alloy. Proc Eng 81:622–627. https://doi.org/10.1016/j.proeng.2014.10.050
22. Schey JA (1987) Introduction to manufacturing processes. McGraw-Hill, New York
23. Qamar S (2010) Shape complexity, metal flow, and dead metal zone in cold extrusion. Mater Manuf Process 25(12):1454–1461. https://doi.org/10.1080/10426914.2010.512650
24. Qamar SZ, Chekotu JC, Al-Maharbi M, Alam K (2019) Shape complexity in metal extrusion: definitions, classification, and applications. Arab J Sci Eng 44:7371–7384. https://doi.org/10.1007/s13369-019-03886-8
25. Fang G, Zhou J, Duszczyk J (2009) Extrusion of 7075 aluminium alloy through double-pocket dies to manufacture a complex profile. J Mater Process Technol 209(6):3050–3059. https://doi.org/10.1016/j.jmatprotec.2008.07.009
26. Wang YL, Song KX, Zhang YM, Wang GX (2019) Microstructure evolution and fracture mechanism of H13 steel during high temperature tensile deformation. Mater Sci Eng, A 746:127–133. https://doi.org/10.1016/j.msea.2019.01.027